Vol. 32 (2001) ACTA PHYSICA POLONICA B No 5

INFLUENCE OF FRACTAL STRUCTURES ON CHAOTIC CRISES AND STOCHASTIC RESONANCE*

A. Krawiecki[a], S. Matyjaśkiewicz[a,b], K. Kacperski[c,a] and J.A. Hołyst[a,b,c]

[a]Faculty of Physics, Warsaw University of Technology
Koszykowa 75, 00-662 Warsaw, Poland
[b]Institute of Physics, Humboldt University at Berlin
Invalidenstraße 110, D-10115 Berlin, Germany
[c]Max Planck Institute for the Physics of Complex Systems
Nöthnitzerstraße 38, D-01187 Dresden, Germany

(Received December 1, 2000)

We present analytical and numerical studies of a chaotic model of a kicked magnetic moment (spin) in the presence of anisotropy and damping. There is an influence of the fractal structure of attractors and basins of attraction on mean transient lifetimes near chaotic crises and on noise-free stochastic resonance in this system. The observed oscillations of average transient times emerging on the background of the well-known power scaling law can be explained by simple geometric models of overlapping fractal sets. Using as the control parameter the amplitude of magnetic field pulses one finds that such measures of stochastic resonance as the input–output correlation function or the signal-to-noise ratio show multiple maxima characteristic of stochastic multiresonance. A simple adiabatic theory which takes into account the fractal structures of this model well explains numerical simulations.

PACS numbers: 05.40.+j, 05.45.+b

1. Introduction

Two-dimensional maps are comfortable tools in the study of deterministic chaos and related nonlinear phenomena, since their dynamics is both rich enough to model complex behavior of physical systems and simple enough to allow fast numerical simulations and analytical treatment. In this paper

* Presented at the XIII Marian Smoluchowski Symposium on Statistical Physics, Zakopane, Poland, September 10–17, 2000.

we use such maps to investigate two related phenomena: crises and noise-free stochastic resonance. A boundary crisis occurs in chaotic systems if a chaotic attractor touches, at a critical value q_c of the control parameter q, a stable manifold of an unstable periodic orbit forming a boundary of the basin of attraction [1, 2]. As the control parameter is further increased the attractor undergoes an abrupt change, *i.e.*, the phase trajectory can penetrate other regions of the parameter space; and the mean transient time $\langle\tau\rangle$ during which the trajectory initiated at a generic point within the former basin of attraction remains close to the precritical attractor obeys the scaling law $\langle\tau\rangle \propto (q - q_\mathrm{c})^\eta$, where η is a critical exponent [1, 2]. On the other hand, Stochastic Resonance (SR) [3–10] is a phenomenon occurring in certain systems driven by a combination of noise and periodic signal, whose essence is that the input noise intensity can be tuned to maximize the degree of periodicity of a properly defined output signal. Noise-free SR is a related phenomenon occurring in chaotic periodically driven systems in which, in the absence of external noise, the internal chaotic dynamics can be changed by varying the control parameter so that the periodic signal is best transmitted [11–18]. It is well known that noise-free SR can be observed in systems with crises due to the presence of a characteristic time $\langle\tau\rangle$ which can be varied with q to match the period of the external drive [11, 14].

In this paper we focus on the effect of the fractal structure of precritical attractors and their basins of attraction on both above-mentioned phenomena. Such a structure may result in the appearance of considerable oscillations of the mean transient time as a function of the control parameter, superimposed on the basic trend given by the above-mentioned scaling law [19, 20]. As a result a periodic signal applied to the system can be equally well transmitted for many different values of the control parameter [21]: *e.g.*, the correlation function between the input (periodic) and output signals becomes a complicated function of q with multiple strong maxima. This is a noise-free counterpart of the effect known as stochastic multiresonance [7, 22, 23] which occurs in certain systems with external noise. Here we present results obtained using a map which models the motion of a damped classical magnetic moment driven by pulses of magnetic field in the presence of anisotropy [19–21,24–26] since in this system the influence of fractal structures on $\langle\tau\rangle$ can be quite strong. We also argue that noise-free stochastic multiresonance occurs in other systems with less visible oscillations of the mean transient time. Our investigations are based on numerical simulations and theoretical calculations. For the latter purpose we use a model of fractal attractor and fractal basin of attraction proposed in Refs. [19, 20] and the adiabatic theory of noise-free SR in the presence of such fractal structures presented in Ref. [21]. Theoretical results explain well both the oscillations of $\langle\tau\rangle$ *vs* q and the multiresonance effect.

2. The model and methods of analysis

We consider a classical magnetic moment (spin) $\boldsymbol{S}$, $|\boldsymbol{S}| = S$ in the uni-axial anisotropy field and external transverse magnetic field $\tilde{B}(t)$ parallel to the x-axis [19–21,24–26], described by the Hamiltonian

$$H = -A\,(S_z)^2 - \tilde{B}\,(t)\,S_x\,, \tag{1}$$

where $A > 0$ is the anisotropy constant. The motion of the spin is determined by the Landau–Lifschitz equation with damping term

$$\frac{d\boldsymbol{S}}{dt} = \boldsymbol{S} \times \boldsymbol{B}_{\text{eff}} - \frac{\lambda}{S}\boldsymbol{S} \times (\boldsymbol{S} \times \boldsymbol{B}_{\text{eff}})\ , \tag{2}$$

where $\boldsymbol{B}_{\text{eff}} = -dH/d\boldsymbol{S}$ is the effective magnetic field and $\lambda > 0$ is the damping parameter. We assume the transverse field in the form of periodic δ-pulses with amplitude B and period $\tilde{\tau}$

$$\tilde{B}\,(t) = B \sum_{n=1}^{\infty} \delta\,(t - n\tilde{\tau})\ . \tag{3}$$

For such a field Eq. (2) can be integrated and the resulting spin dynamics can be written as a superposition of two-dimensional maps T_A and T_B. The map T_A describes the evolution of the spin between kicks and T_B describes the motion of the spin during the action of the field pulses

$$\boldsymbol{S}_{n+1} = T_B\,[T_A\,[\boldsymbol{S}_n]]\,, \tag{4}$$

where $\boldsymbol{S}_n$ is a spin vector just after the action of the n-th magnetic field pulse. A full form of this map can be found in Refs. [21, 24, 26].

The map (4) exhibits a rich variety of chaotic behavior. Let us consider the map (4) with the parameters $S = 1$, $\tilde{\tau} = 2\pi$, $\lambda = 0.1437002$, $A = 1$ and treat B as the control parameter. Then, for B slightly below $B_{\text{c}} = 1.2$ two symmetric chaotic attractors of (4) corresponding to two spin orientations in the absence of the external field exist (spin "up", $S_z > 0$ and "down", $S_z < 0$) [24, 25]. For $B > B_{\text{c}}$ these two attractors merge as a result of the attractor merging crisis [20, 24] and a new post-critical attractor (Fig. 1) consisting of two symmetric parts is born. The system switches chaotically between these two parts. We are interested in the dependence of the mean transient time, which in the case of the attractor merging crisis is the time between consecutive switches [2], on the control parameter. In order to observe noise-free SR we apply the external periodic signal which modulates the control parameter B in Eq. (4) so that it becomes time-dependent

$$B\,(n) = B_0 + B_1 \cos{(\omega_0 n)} \tag{5}$$

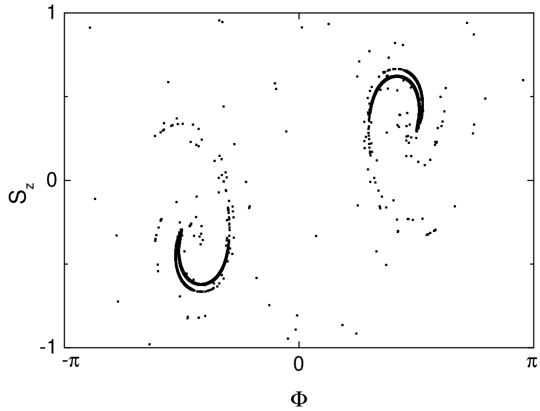

Fig. 1. Attractor of the spin map (4) with $S = 1$, $A = 1$, $\tau = 2\pi$, $\lambda = 0.1437002$, $B_{\rm c} = 1.2$ and $B = 1.2001 > B_{\rm c}$; Φ is the angle between the projection of the spin vector on the x-y plane and the x axis.

and observe its transmission through the system as B_0 is varied. We point out that, contrary to other cases [11, 13], this periodic signal couples to Eq. (4) in a complex (non-additive) manner. The system with such time dependence of the control parameter can be described as a dynamical threshold crossing system and the spin jumps between the two parts of the post-critical attractor can be treated as threshold crossing events [27]. Thus SR can be expected to appear in our system as in other dynamical [8, 12] and non-dynamical [9,10] threshold-crossing systems. We define the output signal y_n as usual in threshold crossing systems, so that one-step long pulses of unit height correspond to the jumps between the two parts of the post-critical attractor: $y_n = 1$ if at iteration n the jump occurred and $y_n = 0$ otherwise. Due to the symmetry of the system with respect to the plane $S_z = 0$ we can assume that the jump occurs when $S_{z,n-1}$ and $S_{z,n}$ have opposite signs (Fig. 2). As a simple measure of the noise-free SR we take the correlation function between the input and output signal

$$C = \frac{\langle y_n B_1 \cos(\omega_0 n)\rangle}{\sqrt{\left(B_1^2/2\right)\left(\langle y_n^2\rangle - \langle y_n\rangle^2\right)}}\,, \tag{6}$$

where the angular brackets denote the time average, and investigate its dependence on B_0. The external signal is best transmitted if C is at a maximum.

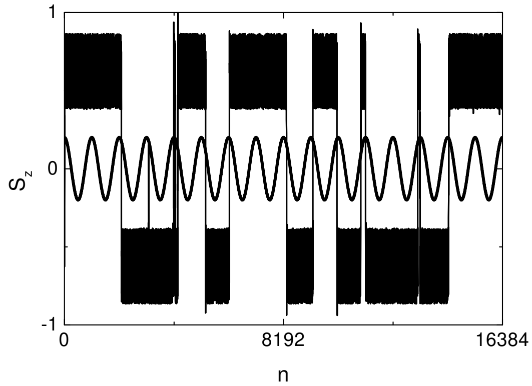

Fig. 2. An example of the time series S_z *vs* n of the spin map (4) with $B_1 = 6 \cdot 10^{-4}$ and $T_0 = 1024$. Also a periodic signal proportional to $B_1 \cos(\omega_0 n)$ is shown. Note that the jumps between the states $S_{z,n} < 0$ and $S_{z,n} > 0$ occur most probably when the periodic signal is at a maximum.

3. Numerical results

3.1. Crisis in the spin map: oscillations of the mean transient time

In Fig. 3 the dependence of the mean transient time $\langle\tau\rangle$ on the control parameter B obtained from numerical simulations of the spin map is shown. Above the crisis at $B_{\rm c} = 1.2$ the power scaling law $\langle\tau(B)\rangle \propto (B - B_{\rm c})^{-\eta}$ with $\eta \approx 0.707$ yields the basic trend of the curve $\langle\tau\rangle$ *vs* B. However, considerable oscillations superimposed on this trend can be also seen. They are a combination of two basic kinds of oscillations, the so-called *normal* and *anomalous* ones.

Above the crisis the precritical attractors are turned into chaotic saddles and their basins into pseudobasins. Just above $B_{\rm c}$ the fractal structure of these new objects can be assumed as identical with that of their precritical counterparts. Normal oscillations appear in chaotic systems in which the precritical basins of attraction do not have a self-similar (fractal) structure. They are induced by consecutive branches of the fractal chaotic saddle creeping, with increasing control parameter, into the non-fractal basin of another precritical attractor [20] which results in the modulation of the slope of the curve $\langle\tau\rangle$ *vs* the control parameter. Anomalous oscillations occur when the precritical basins of attraction are also fractal sets. Their characteristic feature is the presence of sections where the curve $\langle\tau\rangle$ *vs* the control parameter increases against the general trend [19]. Typically their magnitude is larger than that of normal oscillations; *e.g.*, anomalous oscillations are dominating in Fig. 3, but traces of the normal oscillations are also visible.

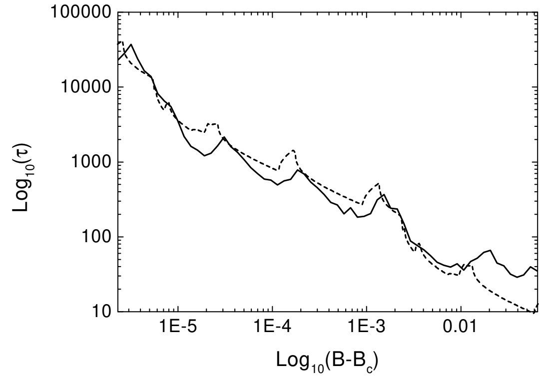

Fig. 3. The mean transient time $\langle\tau\rangle$ *vs* $B-B_{\rm c}$ for the spin map (4) with parameters as in Fig. 1; dominating anomalous oscillations can be seen. Solid line — numerical results; dashed line — theoretical results obtained from the model of Sec. 4.2 with the parameters $\beta=0.124$, $b_E=3.115209\ldots$, $\alpha=0.00234$, $\gamma=0.285$, $b/a=3.83$, $\zeta=1.6$.

3.2. An example of noise-free stochastic multiresonance

In Fig. 4 typical curves C *vs* B_0 are shown for slowly varying input signals with different amplitudes B_1. Jumps between symmetric parts of the postcritical attractor are observed for $B_0>B_{\rm c}-B_1$. Within the range of B_0 shown in Fig. 4 the curves exhibit several strong maxima, so the noise-free stochastic multiresonance is found. These maxima are accompanied by numerous tiny local maxima. We also checked that other measures of SR, like the most popular signal-to-noise ratio (SNR), also exhibit a multi-peaked structure as B_0 is varied [21]. It can be shown that there is a direct correspondence between certain segments of the two curves: $\langle\tau\rangle$ *vs* B and C *vs* B_0+B_1 [21]. This relationship indicates that the occurrence of noise-free stochastic multiresonance and complicated dependence of the correlation function on the control parameter in our model is a result of the fractal structure of precritical attractors and their basins of attraction.

4. Theoretical results

4.1. A model of the fractal chaotic saddle and the pseudobasin

Let us consider a model of a fractal chaotic saddle overlapping a pseudobasin of another, *e.g.*, symmetric chaotic saddle [19, 20]. This model incorporates the important topological properties of the two overlapping sets. The control parameter, which in the spin map (4) should be identified with $B-B_{\rm c}$, will be denoted as q. The time-dependent control parameter will

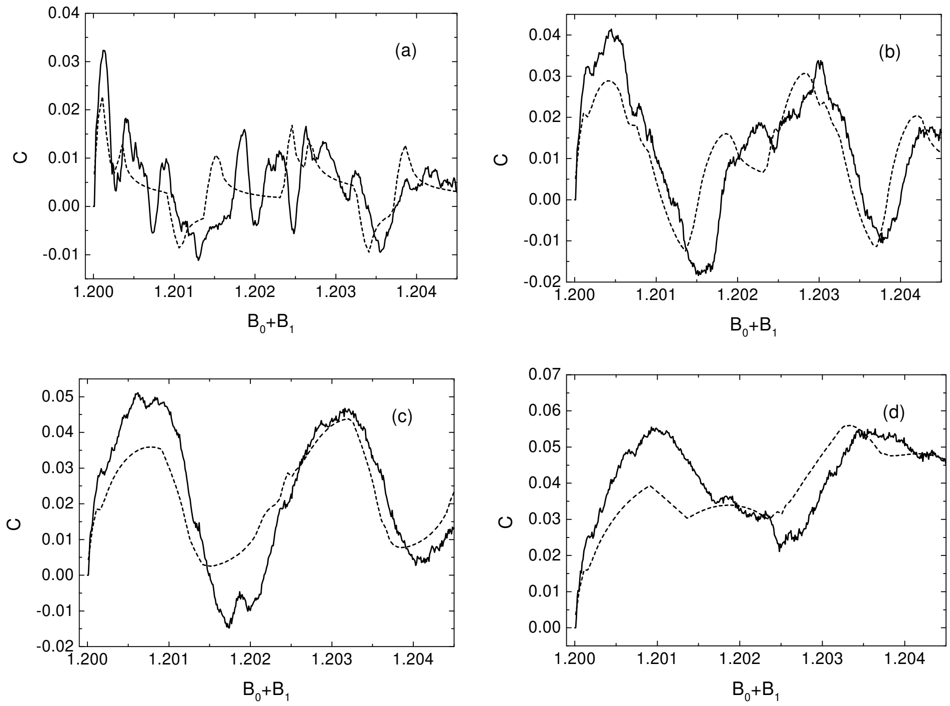

Fig. 4. The correlation function C *vs* B_0 for the signal y_n from the spin map (4) with parameters as in Fig. 1 and $T_0 = 1024$: (a) $B_1 = 1 \cdot 10^{-4}$, (b) $B_1 = 3 \cdot 10^{-4}$, (c) $B_1 = 6 \cdot 10^{-4}$, (d) $B_1 = 1.5 \cdot 10^{-3}$. Solid lines — numerical results; dashed lines — theoretical results obtained from the theory of Sec. 4.3 with the parameters as in Fig. 3.

be denoted as $q\,(n) = q_0 + q_1 \cos(\omega_0 n)$, where q_0 should be identified with $B_0 - B_{\rm c}$ and q_1 with B_1 (*cf.* Eq. (5)).

Let us start with the case of time-independent control parameter q. We assume the model of the chaotic saddle $\mathcal{A}$ as a family of $K+2$ parabolic segments $\mathcal{A}_k$ (Fig. 5)

$$\mathcal{A} = \bigcup_{k=0}^{K+1} \mathcal{A}_k = \bigcup_{k=0}^{K+1} \Big\{ (x,y) : y = -x^2 - (1 - \delta_{k,K+1})\, a\alpha^k + q \Big\}, \qquad (7)$$

where a and α are model parameters. The invariant measure is uniformly distributed along the segments and its relative density on the segment $\mathcal{A}_k$ is assumed as $\tilde{\mu}_k = (1-\gamma)\,\gamma^k$ for $0 \leq k \leq K$ and $\tilde{\mu}_{K+1} = \gamma^{K+1}$, where $0 < \gamma < 1$ is another model parameter. The model of the pseudobasin is

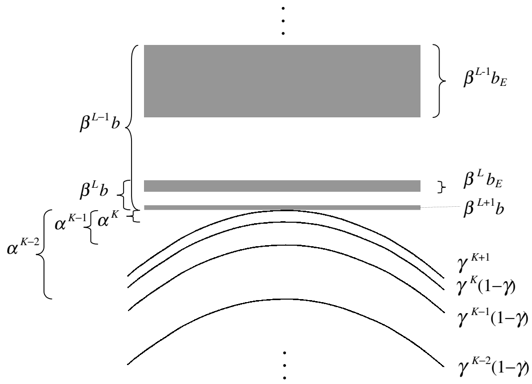

Fig. 5. The model of a fractal chaotic saddle with $a = 1$ and $q = 0$ (7) entering the pseudobasin of attraction of the other saddle (8).

assumed as a family of $L + 2$ stripes $\mathcal{B}_l$ (Fig. 5)

$$\mathcal{B} = \bigcup_{l=0}^{L+1} \mathcal{B}_l = \bigcup_{l=0}^{L+1} \left\{ (x,y) : (1-\delta_{l,L+1}) \left(\beta^l b - \beta^l b_E \right) \leq y \leq \beta^l b \right\} , \qquad (8)$$

where β, b and b_E are again model parameters.

The crisis occurs at $q_{\mathrm{c}} = 0$ when the uppermost parabolic segment of the saddle $\mathcal{A}$ touches the lowermost stripe of the pseudobasin $\mathcal{B}$. All model parameters are determined by the fractal structure of the saddles and pseudobasins of the system under study and can be assessed from magnified plots of the collision region between the chaotic saddles and pseudobasins [19,20]. In order to model the case with the time-dependent control parameter, q should be replaced with $q\,(n)$ in Eqs. (7), (8).

4.2. Theoretical evaluation of the mean transient time

From the model of Sec. 4.1 the mean transient time can be evaluated as $\langle \tau\,(q) \rangle = p^{-1}\,(q)$, where $p\,(q)$ is the probability of jump between the symmetric parts of the post-critical attractor. This probability is proportional to the measure $\mu\,(q)$ of the overlap of the saddle and the pseudobasin of the other saddle [1, 2]. The latter measure is a sum of overlap measures $\mu_{kl}\,(q)$ between the individual parabolic segments $\mathcal{A}_k$ of the chaotic saddle and the stripes $\mathcal{B}_l$ of the pseudobasin. In turn, the quantity $\mu_{kl}\,(q)$ is just the length of the segment $\mathcal{A}_k$ contained inside the stripe $\mathcal{B}_k$ and multiplied by the relative measure density $\tilde{\mu}_k$, thus we obtain

$$p\,(q) = \zeta \mu\,(q) = \zeta \sum_{k=0}^{K+1} \sum_{l=0}^{L+1} \mu_{kl}\,(q) \ , \qquad (9)$$

where ζ is the proportionality constant, and

$$\mu_{kl}(q) = \mu_k\left((1-\delta_{l,L+1})\left(\beta^l b - \beta^l b_E\right), q\right) - \mu_k\left(\beta^l b, q\right) . \qquad (10)$$

In Eq. (10) $\mu_k(c,q)$ denotes the measure of the overlap of the segment $\mathcal{A}_k$ and a half-plane $q > c$ which, for small $q - (1-\delta_{k,K+1})\, a\alpha^k - c$, can be approximated as

$$\mu_k(c,q) = \tilde{\mu}_k \sqrt{q - (1-\delta_{k,K+1})\, a\alpha^k - c}\; \Theta\left(q - a\,(1-\delta_{k,K+1})\,\alpha^k - c\right) , \qquad (11)$$

where $\Theta(\cdot)$ denotes the Heaviside function.

Choosing properly the model parameters (their values are given below Fig. 3) one can reproduce the complicated dependence of the mean transient time on the control parameter with high accuracy (Fig. 3). In particular, the anomalous and normal oscillations of $\langle \tau(q) \rangle$ are reproduced. Using certain simplifications of the above model it is possible to obtain simple analytic expressions for the period and magnitude of normal oscillations [20] and for the period and maximum height of anomalous oscillations [19, 20] which agree well with numerical results.

4.3. Theoretical evaluation of the correlation function

In the case of the time-dependent control parameter $q(n) = q_0 + q_1 \cos(\omega_0 n)$ the jump probability $p(q(n)) \equiv p(n)$ becomes also time-dependent. Then, in the continuous time approximation, and taking into account that $y_n^2 = y_n$, it can be easily shown that

$$\langle y_n B_1 \cos(\omega_0 n) \rangle = T_0^{-1} \int_0^{T_0} p(t)\, B_1 \cos(\omega_0 t)\, dt = B_1 P_1(q_0) , \qquad (12)$$

$$\langle y_n^2 \rangle = \langle y_n \rangle = T_0^{-1} \int_0^{T_0} p(t)\, dt = \overline{p(q_0)} , \qquad (13)$$

where $T_0 = 2\pi/\omega_0$ is the period of external signal, P_1 is the first Fourier coefficient, and $\overline{p}$ is the mean value over T_0 of $p(t)$. If the external periodic signal is slowly varying in time, the adiabatic approximation can be used [6] in which the time-dependent jump probability can be obtained from our model by replacing q with $q(n)$ in Eqs. (9)–(11). Then, the quantities P_1 and $\overline{p}$ can be evaluated analytically, and the resulting expressions are double sums similar to that in Eq. (9), containing complicated combinations of elliptic integrals of the first and second kind. The complete expressions for P_1 and $\overline{p}$ can be found in Ref. [21].

Choosing the same set of model parameters which enabled us to fit the theoretical and numerical curves of the mean transient time *vs* the control parameter in Sec. 4.2 we obtained the theoretical curves C *vs* q_0 shown in Fig. 4. In Figs. 4(b)–(d), *i.e.*, for larger values of the amplitude B_1, the agreement between the theoretical and numerical results is good. Not only the multiresonance effect is found, *i.e.*, the maximization of the input–output correlation function for many values of the control parameter, but also the location and height of the maxima of C are predicted quite well. In Fig. 4(a) only qualitative agreement between the theoretical and numerical curves can be seen. This is connected with the fact that in our model (7), (8) we neglect further splitting of the parabolic segments and stripes with small indices k and l, respectively. This splitting, however, occurs in a real system and causes the increase of the number of maxima of C and shift of their location in comparison with the theoretical prediction. The above results thus prove that the appearance of noise-free stochastic multiresonance is a direct consequence of the fractal structure of precritical attractors and their basins. They also show that for slowly varying periodic signals this effect can be at least qualitatively explained using the adiabatic approximation for the time-dependent probabilities $p\,(n)$.

5. Discussion and conclusions

In this paper we discussed two effects connected with the influence of the fractal structure of precritical attractors and their basins of attraction on the dynamics of system near crises: oscillations of the mean transient time and noise-free stochastic multiresonance. The former effect has long been known [2, 28], however, it has been treated as a rather small deviation from the basic power scaling of $\langle\tau\rangle$ and not studied in detail. Only recently analytic theory of this effect has been elaborated by two of us [19, 20]. Our further work has shown that if SR is investigated in a system close to crisis, the fractality of precritical attractors and their basins leads to a more spectacular effect of noise-free stochastic multiresonance, which cannot be treated as a small deviation from the typical picture of SR with a single maximum of C or SNR [21]. It should be emphasized that both effects appear naturally in our system, while, *e.g.*, the appearance of stochastic multiresonance in a system with noise required a purposeful construction of a multistable potential [22, 23].

The fine structure of precritical attractors and their basins is best reflected in the numerous maxima of C for a very small amplitude of the periodic signal (Fig. 4(a)). As B_1 is increased the details of the fractal structure smaller than *ca.* $2B_1$ are averaged and the curve C *vs* B_0 is smoothed out. For small B_1, tiny (*i.e.*, on the order of B_1) changes of the control parameter B_0 lead to dramatic changes of C, *i.e.*, of the quality of signal transmission. This important effect usually cannot be found in typical systems with SR where the maxima of C or the SNR are smooth and soft (including chaotic one-dimensional maps in which noise-free SR can be observed [11–13]). Hence large sensitivity of SR to small changes of the control parameter can be considered as typical of systems with oscillations of the mean transient time.

In our study of SR in this work we used as a measure the input–output correlation function instead of the most popular SNR. It can be shown that also the SNR exhibits multiple maxima as the control parameter is varied [21]. We observed better agreement between numerical and theoretical curves C *vs* B_0 than SNR *vs* B_0. This is probably since in order to evaluate C using the theory of Sec. 4.3 only the adiabatic approximation is needed, while in order to evaluate the SNR analytically one should make additional assumptions concerning the statistical independence of the jumps between symmetric parts of the postcritical attractor [10, 21].

So far, we have discussed noise-free stochastic multiresonance only in a system with fractal basins of precritical attractors. However, the presence of strong anomalous oscillations of $\langle\tau\rangle$ is not a necessary condition for the occurrence of many maxima of the correlation function or the SNR. Our preliminary results obtained in systems in which normal oscillations of the mean transient time are dominating confirm this conclusion; a full account of these results will be published elsewhere. Since oscillations of the mean transient time are often observed in systems with crises [2, 28] noise-free stochastic multiresonance should be also observable in many such systems, including experimental ones with continuous time.

REFERENCES

[1] C. Grebogi, E. Ott, J.A. Yorke, *Phys. Rev. Lett.* **57**, 1284 (1986).

[2] C. Grebogi, E. Ott, F. Romeiras, J.A. Yorke, *Phys. Rev.* **A36**, 5365 (1987).

[3] R. Benzi, A. Sutera, A. Vulpiani, *J. Phys. A* **14**, L453 (1981).

[4] L. Gammaitoni, P. Hänggi, P. Jung, F. Marchesoni, *Rev. Mod. Phys.* **70**, 223 (1998).

[5] V.S. Anischenko, A.B. Neiman, F. Moss, L. Schimansky-Geier, *Phys. Usp.* **42**, 7 (1999), [*Usp. Fiz. Nauk* **169**, 7 (1999)].

[6] B. McNamara, K. Wiesenfeld, *Phys. Rev.* **A39**, 4854 (1989).

[7] P. Jung, P. Hänggi, *Phys. Rev.* **A44**, 8032 (1991).

[8] K. Wiesenfeld, D. Pierson, E. Pantazelou, Ch. Dames, F. Moss, *Phys. Rev. Lett.* **78**, 2882 (1997).
[9] Z. Gingl, L.B. Kiss, F. Moss, *Europhys. Lett.* **29**, 191 (1995).
[10] F. Chapeau-Blondeau, *Phys. Rev.* **E53**, 5469 (1996).
[11] V. S. Anishchenko, A. B. Neiman, M.A. Safanova, *J. Stat. Phys.* **70**, 183 (1993).
[12] A. Krawiecki, A. Sukiennicki, *Chaos* **8**, 768 (1998).
[13] S. Sinha, B.K. Chakrabarti, *Phys. Rev.* **E58**, 8009 (1998).
[14] T.L. Carroll, L.M. Peccora, *Phys. Rev. Lett.* **70**, 576 (1993).
[15] A. Crisanti, M. Falcioni, G. Paladin, A. Vulpiani, *J. Phys. A* **27**, L597 (1994).
[16] V.S. Anishchenko, M.A. Safonova, L.O. Chua, *Int. J. Bifurcation* & *Chaos* **4**, 441 (1994).
[17] E. Reibold, W. Just, J. Becker, H. Benner, *Phys. Rev. Lett.* **78**, 3101 (1997).
[18] W. Wang, Z.D. Wang, *Phys. Rev.* **E55**, 7379 (1997).
[19] K. Kacperski, J.A. Hołyst, *Phys. Lett.* **A254**, 53 (1999).
[20] K. Kacperski, J.A. Hołyst, *Phys. Rev.* **E60**, 403 (1999).
[21] S. Matyjaśkiewicz, A. Krawiecki, J.A. Hołyst, K. Kacperski, W. Ebeling, to appear in *Phys. Rev.* **E**.
[22] J.M.G. Vilar, J.M. Rubí, *Phys. Rev. Lett.* **78**, 2882 (1997).
[23] J.M.G. Vilar, J.M. Rubí, *Physica* **A264**, 1 (1999).
[24] J.A. Hołyst, A. Sukiennicki, *Acta Phys. Pol.* **A81**, 353 (1992).
[25] J.A. Hołyst, A. Sukiennicki, *J. Magn. Magn. Mater.* **104-107**, 2111 (1992).
[26] K. Kacperski, J. A. Hołyst, *Phys. Rev.* **E55**, 5044 (1997).
[27] S. Matyjaśkiewicz, J.A. Hołyst, A. Krawiecki, *Phys. Rev.* **E61**, 5134 (2000).
[28] J.C. Sommerer, C. Grebogi, *Int. J. Bifurcation* & *Chaos Appl. Sci. Eng.* **2**, 383 (1992).